Cosmological family asymmetry and CP violation

T. Fujihara,[1,*] S. Kaneko,[2,†] S. Kang,[3,‡] D. Kimura,[1,§] T. Morozumi,[1,∥] and M. Tanimoto[4,¶]

[1]*Graduate School of Science, Hiroshima University, Higashi-Hiroshima, Japan, 739-8526*

[2]*Department of Physics, Ochanomizu University, Tokyo, Japan 112-8610*

[3]*Seoul National University, Seoul, Korea 151-734*

[4]*Department of Physics, Niigata University, Niigata, Japan 950-2181*

(Received 12 May 2005; published 27 July 2005)

We discuss how the cosmological baryon asymmetry can be achieved by the lepton family asymmetries of heavy Majorana neutrino decays and how the lepton family asymmetries are related to CP violation in neutrino oscillation, in the minimal seesaw model with two heavy Majorana neutrinos. We derive the most general formula for CP violation in neutrino oscillation in terms of the heavy Majorana masses and Yukawa mass term. It is shown that the formula is very useful to classify several models in which e, μ, and τ leptogenesis can be separately realized and to see how they are connected with low energy CP violation. To make the models predictive, we take texture with two zeros in the Dirac matrix. In particular, we find some interesting cases in which CP violation in neutrino oscillation can happen while lepton family asymmetries do not exist at all. On the contrary, we can find e-, μ-, and τ-leptogenesis scenarios in which the cosmological CP violation and low energy CP violation measurable via neutrino oscillations are very closely related to each other. By determining the allowed ranges of the parameters in the models, we predict the sizes of CP violation in neutrino oscillation and $|V_{e3}^{\mathrm{MNS}}|$. Finally, the leptonic unitarity triangles are reconstructed.

DOI: 10.1103/PhysRevD.72.016006 PACS numbers: 11.30.Cp, 11.30.Fs, 12.15.Ff

I. INTRODUCTION

CP violations in the neutrino seesaw models have recently attracted much attention because the measurements of CP violation via neutrino oscillation are being planned in future experiments and there may exist a connection between the low energy neutrino CP violation and the matter and antimatter asymmetry of the Universe through the leptogenesis scenario in the seesaw models [1]. In contrast to the quark sector, since the number of independent CP violating phases in the neutrino seesaw models is more than 1 [2], it is not straightforward to discriminate the CP violating phases contributing to the leptogenesis from the low energy experiments [3]. One can show that the CP violation phases at high energy can contribute to the low energy effective Majorana mass matrix and thus they may be concerned with a CP violating phase called δ in the standard parametrization of the Maki, Nakagawa, and Sakata (MNS) matrix, which is measurable from CP violation in neutrino oscillation. One might think that nonzero δ may play a role in CP violation for leptogenesis in the neutrino seesaw models. However, this is not always the case, because several independent CP phases contribute to both the leptogenesis CP violation at high energy and CP violation of neutrino oscillation at low energy. There is the case in which at low energy the total effect of many CP phases are canceled, but at high energy cosmological CP violation remains. There is the opposite case in which the cosmological CP violation vanishes while CP violation at low energy is nonzero. Considering the situation, it is important to study CP violation phenomena as much as possible both at high energy and low energy.

In the previous work [4], it was shown that the lepton family asymmetries Y_e, Y_μ, and Y_τ which are generated by heavy Majorana neutrino decays are sensitive to one of the many CP violating phases. Though the total lepton asymmetry $Y = Y_e + Y_\mu + Y_\tau$ remains as a constant, flavor composition of the asymmetries $Y_e{:}Y_\mu{:}Y_\tau$ can vary by changing the phase. As a particularly interesting case, the amount and the sign of each lepton family asymmetry Y_i can be very different from the total lepton asymmetry as $|Y| \ll |Y_\mu|, |Y_\tau|$. One can also find the case [4] where the lepton asymmetry Y could be dominated by a particular lepton family asymmetry as $Y \sim Y_\mu$ or $Y \sim Y_\tau$. If this is the case, it indicates the interesting scenario of baryogenesis that the matter in the present universe was originated by the second or the third family of leptons. Interestingly, the models proposed in [5] correspond to the μ or τ family number dominant leptogenesis scenarios. In this work, we study how such a scenario can be probed by low energy flavor violating processes such as neutrino oscillations.

The paper is organized as follows. In Sec. II, we study how CP violating phases are related to lepton family asymmetries. The reason why, in general, the family asymmetries can be different from the total lepton number asymmetry is shown in a comprehensive way. Then we show how they have some impact on the CP violation in the neutrino mixings by deriving the formula for low

*Email address: fujihara@theo.phys.sci.hiroshima-u.ac.jp
†Email address: sotoru@phys.ocha.ac.jp
‡Email address: skkang@phya.snu.ac.kr
§Email address: kimura@theo.phys.sci.hiroshima-u.ac.jp
∥Email address: morozumi@hiroshima-u.ac.jp
¶Email address: tanimoto@muse.sc.niigata-u.ac.jp

energy CP violation neutrino mixings in terms of the fundamental parameters for the minimal seesaw model. In Sec. III, we focus on the textures with two zeros in Yukawa mass terms. The analytical formulas for the MNS matrix are given both for normal and inverted cases. In Sec. IV, by using the mixing angles and mass squared differences determined by neutrino oscillation experiments, we determine the parameters of the models and make prediction on $|V_{e3}^{\rm MNS}|$ and CP violation in neutrino oscillation. Based on this numerical fit, we reconstruct the leptonic unitarity triangles. Section V is devoted to summary and discussion.

II. *CP* VIOLATION RELATED TO THE LEPTON FAMILY ASYMMETRY

We start with the lepton family asymmetries generated from heavy Majorana neutrino decays, which are defined by [4,6]

$$\epsilon_i^k = \frac{\Gamma[N^k \to l_i^- \phi^+] - \Gamma[N^k \to l_i^+ \phi^-]}{\Gamma[N^k \to l_i^- \phi^+] + \Gamma[N^k \to l_i^+ \phi^-]}, \tag{1}$$

where $i = (e, \mu, \tau)$ and N^k denotes kth heavy Majorana neutrino. The total lepton number asymmetry from N^k is [1]

$$\epsilon^k = \sum_{i=e,\mu,\tau} \epsilon_i^k \mathrm{Br}(N^k \to l_i^{\pm} \phi^{\mp}), \tag{2}$$

where Br denotes the tree level branching fraction. For our purpose, let us focus on the seesaw model with two heavy Majorana neutrinos [5,7–10],

$$\mathcal{L}_m = -y_\nu^{ik} \overline{L}_i N_k \tilde{\phi} - y_l^i \overline{L}_i l_{R_i} \phi - \frac{1}{2} \overline{N}_k{}^c M_k N_k + \text{h.c.}, \tag{3}$$

where $i = e, \mu, \tau$ and $k = 1, 2$. L_i, l_R, ϕ are $SU(2)$ lepton doublet fields, charged lepton singlet fields, and Higgs scalar, respectively. Here we take a basis in which both charged lepton and singlet Majorana neutrino mass matrices are real and diagonal. In this basis, the lepton family asymmetries given in Eq. (1) can be written as [4]

$$\epsilon_i^k = \frac{1}{8\pi} \sum_{k' \neq k} \left[I(x_{k'k}) \frac{\mathrm{Im}[(y_\nu^\dagger y_\nu)_{kk'} (y_\nu)_{ik}^* (y_\nu)_{ik'}]}{|(y_\nu)_{ik}|^2} + \frac{1}{1 - x_{k'k}} \frac{\mathrm{Im}[(y_\nu^\dagger y_\nu)_{k'k} (y_\nu)_{ik}^* (y_\nu)_{ik'}]}{|(y_\nu)_{ik}|^2} \right], \tag{4}$$

where $x_{k'k} = M_{k'}^2 / M_k^2$ and $I(x)$ is given as [1,11]

$$I(x) = \sqrt{x} \left[1 + \frac{1}{1-x} + (1+x) \ln \frac{x}{1+x} \right] = \begin{cases} -\frac{3}{2} x^{-1/2} & \text{for } x \gg 1, \\ -2x^{3/2} & \text{for } x \ll 1. \end{cases} \tag{5}$$

It is convenient to write 3×2 Dirac mass matrix $m_D = y_\nu \frac{v}{\sqrt{2}}$ as

$$m_D = (\mathbf{m_{D1}}, \mathbf{m_{D2}}) = \begin{pmatrix} m_{De1} & m_{De2} \\ m_{D\mu 1} & m_{D\mu 2} \\ m_{D\tau 1} & m_{D\tau 2} \end{pmatrix} = (\mathbf{u_1}, \mathbf{u_2}) \begin{pmatrix} m_{D1} & 0 \\ 0 & m_{D2} \end{pmatrix}, \tag{6}$$

where two unit vectors are introduced,

$$\mathbf{u_k} = \frac{\mathbf{m_{Dk}}}{m_{Dk}}, \tag{7}$$

with $m_{Dk} = |\mathbf{m_{Dk}}|$. Without loss of generality, we can take $\mathbf{u_1}$ and $\mathbf{u_2}$ to be real and complex, respectively. Then, three CP violating phases correspond to $\arg(u_{i2})$ ($i = e$, μ, and τ). With the definitions, one can write

$$\begin{aligned} &\mathrm{Br}(N^k \to l_i^{\mp} \phi^{\pm}) = |u_{ik}|^2, \\ &\epsilon_i^1 \mathrm{Br}(N^1 \to l_i^{\mp} \phi^{\pm}) = \frac{(m_{D2})^2}{4\pi v^2} \left(I\left(\frac{M_2^2}{M_1^2}\right) \mathrm{Im}[(\mathbf{u_1^\dagger} \cdot \mathbf{u_2}) u_{i1}^* u_{i2}] + \frac{M_1^2}{M_1^2 - M_2^2} \mathrm{Im}[(\mathbf{u_1^\dagger} \cdot \mathbf{u_2})^* u_{i1}^* u_{i2}] \right), \\ &\epsilon_i^2 \mathrm{Br}(N^2 \to l_i^{\mp} \phi^{\pm}) = -\frac{(m_{D1})^2}{4\pi v^2} \left(I\left(\frac{M_1^2}{M_2^2}\right) \mathrm{Im}[(\mathbf{u_1^\dagger} \cdot \mathbf{u_2}) u_{i1}^* u_{i2}] + \frac{M_2^2}{M_2^2 - M_1^2} \mathrm{Im}[(\mathbf{u_1^\dagger} \cdot \mathbf{u_2})^* u_{i1}^* u_{i2}] \right). \end{aligned} \tag{8}$$

It is interesting to note that the lepton family asymmetries are related to the following combinations of Yukawa terms,

$$A_{12}^e = (\mathbf{u_1^\dagger} \cdot \mathbf{u_2}) u_{e1}^* u_{e2}, \qquad A_{12}^\mu = (\mathbf{u_1^\dagger} \cdot \mathbf{u_2}) u_{\mu 1}^* u_{\mu 2}, \qquad A_{12}^\tau = (\mathbf{u_1^\dagger} \cdot \mathbf{u_2}) u_{\tau 1}^* u_{\tau 2}, \tag{9}$$

$$B_{12}^e = (\mathbf{u_1^\dagger} \cdot \mathbf{u_2})^* u_{e1}^* u_{e2}, \qquad B_{12}^\mu = (\mathbf{u_1^\dagger} \cdot \mathbf{u_2})^* u_{\mu 1}^* u_{\mu 2}, \qquad B_{12}^\tau = (\mathbf{u_1^\dagger} \cdot \mathbf{u_2})^* u_{\tau 1}^* u_{\tau 2}, \tag{10}$$

where $A_{12}^i = B_{12}^i \exp(2i\gamma)$ with $\gamma = \arg(\mathbf{u_1^\dagger} \cdot \mathbf{u_2})$. In addition, A_{12} and B_{12} satisfy the following sum rules,

$$\begin{aligned} A_{12}^e + A_{12}^\mu + A_{12}^\tau &= (\mathbf{u_1^\dagger} \cdot \mathbf{u_2})^2, \\ B_{12}^e + B_{12}^\mu + B_{12}^\tau &= |(\mathbf{u_1^\dagger} \cdot \mathbf{u_2})|^2. \end{aligned} \tag{11}$$

The relations are shown in Fig. 1, where $\gamma = \frac{\pi}{4}$ is taken. They are quadrangles in a complex plane. The imaginary part of A is related to CP asymmetry of leptogenesis. The ratios of lepton family asymmetry to the total lepton asym-

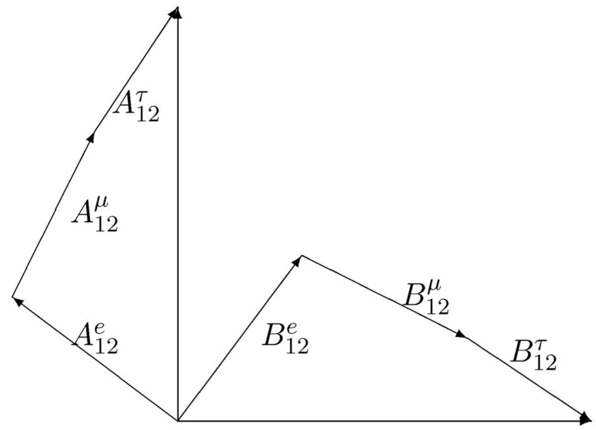

FIG. 1. Schematic view of quadrangles.

metry are written as

$$\frac{\epsilon_i^1}{\epsilon^1} = \frac{I(M_2^2/M_1^2)\mathrm{Im}A_{12}^i + [M_1^2/(M_1^2 - M_2^2)]\mathrm{Im}B_{12}^i}{I(M_2^2/M_1^2)(\mathrm{Im}A_{12}^e + \mathrm{Im}A_{12}^{\mu} + \mathrm{Im}A_{12}^{\tau})},$$
$$\frac{\epsilon_i^2}{\epsilon^2} = \frac{I(M_1^2/M_2^2)\mathrm{Im}A_{21}^i + [M_2^2/(M_2^2 - M_1^2)]\mathrm{Im}B_{21}^i}{I(M_1^2/M_2^2)(\mathrm{Im}A_{21}^e + \mathrm{Im}A_{21}^{\mu} + \mathrm{Im}A_{21}^{\tau})}. \tag{12}$$

In the model with two heavy Majorana neutrinos N_1 and N_2 with large hierarchical mass, e.g., $M_1 \ll M_2$, the family asymmetries from the lightest heavy Majorana neutrinos decay are approximately given as

$$\frac{\epsilon_e^1}{\epsilon^1} \approx \frac{\mathrm{Im}A_{12}^e}{\mathrm{Im}(A_{12}^e + A_{12}^{\mu} + A_{12}^{\tau})},$$
$$\frac{\epsilon_{\mu}^1}{\epsilon^1} \approx \frac{\mathrm{Im}A_{12}^{\mu}}{\mathrm{Im}(A_{12}^e + A_{12}^{\mu} + A_{12}^{\tau})}, \tag{13}$$
$$\frac{\epsilon_{\tau}^1}{\epsilon^1} \approx \frac{\mathrm{Im}A_{12}^{\tau}}{\mathrm{Im}(A_{12}^e + A_{12}^{\mu} + A_{12}^{\tau})}.$$

Therefore one-family dominant leptogenesis can be realized when the quadrangle is replaced by a line which is determined by one of A_{12}^e, A_{12}^{μ}, and A_{12}^{τ} with a nontrivial *CP* violating phase. If this is the case, the imaginary parts of A_{12}^e, A_{12}^{μ}, and A_{12}^{τ} are related to e leptogenesis, μ leptogenesis, and τ leptogenesis, respectively. We also note that the imaginary part of $\sum_i A^i$ can be smaller than the imaginary part of A^i. If this is the case, each family asymmetry is much larger than the total lepton asymmetry. Now let us discuss how the family asymmetry is related to the *CP* violation in neutrino oscillations,

$$P(\nu_{\mu} \to \nu_e) - P(\bar{\nu}_{\mu} \to \bar{\nu}_e) = 4J\left(\sin\frac{\Delta m_{12}^2 L}{2E} + \sin\frac{\Delta m_{23}^2 L}{2E} + \sin\frac{\Delta m_{31}^2 L}{2E}\right), \tag{14}$$

where J is the Jarlskog invariant [12] defined as

$$J = \mathrm{Im}(V_{e1}^{\mathrm{MNS}} V_{\mu 1}^{\mathrm{MNS}*} V_{e2}^{\mathrm{MNS}*} V_{\mu 2}^{\mathrm{MNS}}). \tag{15}$$

In the basis where the charged lepton mass matrix is diagonal, J is related to the following quantity [3],

$$\Delta = \mathrm{Im}((m_{\mathrm{eff}} m_{\mathrm{eff}}^{\dagger})_{e\mu} (m_{\mathrm{eff}} m_{\mathrm{eff}}^{\dagger})_{\mu\tau} (m_{\mathrm{eff}} m_{\mathrm{eff}}^{\dagger})_{\tau e}), \tag{16}$$

where $m_{\mathrm{eff}} = -m_D \frac{1}{M} m_D^T$, and the relation between J and Δ is given as

$$J = \frac{\Delta}{(n_1^2 - n_2^2)(n_2^2 - n_3^2)(n_3^2 - n_1^2)}, \tag{17}$$

where n_j^2 are three mass eigenvalues of $m_{\mathrm{eff}} m_{\mathrm{eff}}^{\dagger}$. To facilitate the calculation of Δ, we introduce three 2×2 Hermitian matrices H_e, H_{μ}, and H_{τ},

$$H_i = \begin{pmatrix} \frac{|m_{Di1}|^2}{M_1} & \frac{m_{Di1} m_{Di2}^*}{\sqrt{M_1 M_2}} \\ \frac{m_{Di1}^* m_{Di2}}{\sqrt{M_1 M_2}} & \frac{|m_{Di2}|^2}{M_2} \end{pmatrix}, \quad (i = e, \mu, \tau), \tag{18}$$

and Δ is obtained by simply taking trace of the product of Hs,

$$\Delta = \mathrm{Im}\,\mathrm{Tr}(H^* H_e H^* H_{\mu} H^* H_{\tau}), \tag{19}$$

with $H = H_e + H_{\mu} + H_{\tau}$. The formula given in terms of 2×2 matrices H is useful and can be generalized to the seesaw model including any number (n_M) of heavy Majorana neutrinos by replacing 2×2 matrices H in Eq. (18) by $n_M \times n_M$ matrices. Equation (19) shows that *CP* violation in neutrino oscillation is related to the imaginary part of H_{e12}, $H_{\mu 12}$, and $H_{\tau 12}$. We introduce the following parameters with mass dimension,

$$X_k = \frac{m_{Dk}^2}{M_k}, \quad (k = 1, 2). \tag{20}$$

By substituting Eq. (18) into Eq. (19), we obtain

$$\begin{aligned}\Delta = {}& (1 - |\mathbf{u_1^{\dagger}} \cdot \mathbf{u_2}|^2)(X_1^4 X_2^2 (\mathrm{Im}[(u_{e1}^* u_{e2} u_{\mu 1} u_{\mu 2}^*)|u_{\tau 1}|^2 + (u_{\mu 1}^* u_{\mu 2} u_{\tau 1} u_{\tau 2}^*)|u_{e1}|^2 + (u_{\tau 1}^* u_{\tau 2} u_{e1} u_{e2}^*)|u_{\mu 1}|^2]) \\ & + X_1^3 X_2^3 (\mathrm{Im}[(u_{e1}^* u_{e2})(\mathbf{u_1^{\dagger}} \cdot \mathbf{u_2})(|u_{\tau 1} u_{\mu 2}|^2 - |u_{\mu 1} u_{\tau 2}|^2) + (u_{\mu 1}^* u_{\mu 2})(\mathbf{u_1^{\dagger}} \cdot \mathbf{u_2})(|u_{e1} u_{\tau 2}|^2 - |u_{\tau 1} u_{e2}|^2) \\ & + (u_{\tau 1}^* u_{\tau 2})(\mathbf{u_1^{\dagger}} \cdot \mathbf{u_2})(|u_{\mu 1} u_{e2}|^2 - |u_{e1} u_{\mu 2}|^2)]) - X_1^2 X_2^4 (\mathrm{Im}[(u_{e1}^* u_{e2} u_{\mu 1} u_{\mu 2}^*)|u_{\tau 2}|^2 + (u_{\mu 1}^* u_{\mu 2} u_{\tau 1} u_{\tau 2}^*)|u_{e2}|^2 \\ & + (u_{\tau 1}^* u_{\tau 2} u_{e1} u_{e2}^*)|u_{\mu 2}|^2])).\end{aligned} \tag{21}$$

This is the most general formula to express the low energy *CP* violation measurable via neutrino oscillation in terms of the Majorana masses and the Yukawa terms in the seesaw model and a main result of the paper. In the model with two heavy Majorana neutrinos, the same quantity is computed for two zero texture models in [5]. For the most general case, J is

TABLE I. Type I texture models and low energy CP violation.

Type		Δ
Type I(a) e leptogenesis	$\begin{pmatrix} u_{e1} & u_{e2} \\ u_{\mu 1} & 0 \\ 0 & u_{\tau 2} \end{pmatrix}$	$(1-\lvert u_{e1}u_{e2}\rvert^2)X_1^3X_2^3\,\mathrm{Im}(u_{e1}^*u_{e2})^2(-\lvert u_{\tau 2}\rvert^2\lvert u_{\mu 1}\rvert^2)$
Type I(b) e leptogenesis	$\begin{pmatrix} u_{e1} & u_{e2} \\ 0 & u_{\mu 2} \\ u_{\tau 1} & 0 \end{pmatrix}$	$(1-\lvert u_{e1}u_{e2}\rvert^2)X_1^3X_2^3\,\mathrm{Im}(u_{e1}^*u_{e2})^2\lvert u_{\tau 1}\rvert^2\lvert u_{\mu 2}\rvert^2.$
Type I(a) μ leptogenesis	$\begin{pmatrix} u_{e1} & 0 \\ u_{\mu 1} & u_{\mu 2} \\ 0 & u_{\tau 2} \end{pmatrix}$	$(1-\lvert u_{\mu 1}u_{\mu 2}\rvert^2)X_1^3X_2^3\,\mathrm{Im}(u_{\mu 1}^*u_{\mu 2})^2(\lvert u_{\tau 2}\rvert^2\lvert u_{e1}\rvert^2)$
Type I(b) μ leptogenesis	$\begin{pmatrix} 0 & u_{e2} \\ u_{\mu 1} & u_{\mu 2} \\ u_{\tau 1} & 0 \end{pmatrix}$	$(1-\lvert u_{\mu 1}u_{\mu 2}\rvert^2)X_1^3X_2^3\,\mathrm{Im}(u_{\mu 1}^*u_{\mu 2})^2(-\lvert u_{e2}\rvert^2\lvert u_{\tau 1}\rvert^2)$
Type I(a) τ leptogenesis	$\begin{pmatrix} u_{e1} & 0 \\ 0 & u_{\mu 2} \\ u_{\tau 1} & u_{\tau 2} \end{pmatrix}$	$(1-\lvert u_{\tau 1}u_{\tau 2}\rvert^2)X_1^3X_2^3\,\mathrm{Im}(u_{\tau 1}^*u_{\tau 2})^2(-\lvert u_{e1}\rvert^2\lvert u_{\mu 2}\rvert^2)$
Type I(b) τ leptogenesis	$\begin{pmatrix} 0 & u_{e2} \\ u_{\mu 1} & 0 \\ u_{\tau 1} & u_{\tau 2} \end{pmatrix}$	$(1-\lvert u_{\tau 1}u_{\tau 2}\rvert^2)X_1^3X_2^3\,\mathrm{Im}(u_{\tau 1}^*u_{\tau 2})^2(\lvert u_{e2}\rvert^2\lvert u_{\mu 1}\rvert^2)$

obtained by using bi-unitary parametrization of m_D [7]. It is worthwhile to note that the terms proportional to $X_1^3X_2^3$ are related to the family asymmetries because they are proportional to $\mathrm{Im}A_{12}^e$, $\mathrm{Im}A_{12}^\mu$, and $\mathrm{Im}A_{12}^\tau$. However, the terms proportional to $X_1^4X_2^2$ and $X_1^2X_2^4$ are not directly related to $\mathrm{Im}A^i$. Now, let us study the following two interesting cases.

(1) $\mathbf{u_1^\dagger}\cdot\mathbf{u_2}=0$.

This corresponds to the case that there is no leptogenesis and any family asymmetries are vanishing. However, CP violation in neutrino oscillation can occur in this case because Δ is not vanishing,

$$\Delta = X_1^2X_2^2(X_1^2-X_2^2)\mathrm{Im}(u_{\tau 1}^*u_{\tau 2}u_{e1}u_{e2}^*). \tag{22}$$

(2) $\mathbf{u_1^\dagger}\cdot\mathbf{u_2}=u_{a1}^*u_{a2}$ $(a=e,\mu,\tau)$.

Each case for a corresponds to one-family dominant leptogenesis, such as e leptogenesis, μ letogenesis, or τ leptogenesis. This implies that the lepton asymmetry is dominated by one particular family asymmetry. In order to see how the scenarios of leptogenesis are connected with the low energy CP violation parametrized by Δ, we consider the Dirac neutrino Yukawa matrix containing two zeros which makes the scenarios more predictable. In this class of the models, the light neutrino mass matrix given by m_{eff} can be parametrized by five independent parameters. From the experimental results on three mixing angles and two mass squared differences, the five parameters including a CP phase are strongly constrained. In Tables I and II, we classify the models with two zeros texture into type I and II depending on the positions of the two zeros in the neutrino Dirac Yukawa matrix. As one can see from Table I, for type I models, Δ is generally nonvanishing and proportional to $\mathrm{Im}(u_{a1}^*u_{a2})^2$, which implies that there exists a strong correlation between low energy CP violation and leptogenesis. In contrast to the type I models, for the type II models, the low energy CP violating parameter Δ is vanishing and thus it is difficult to trace the origin of cosmological family asymmetries from the measurement of the CP violation in neutrino oscillation.

TABLE II. Type II texture models and the MNS matrix.

Type	(a)	(b)	$V^{\mathrm{MNS}N}$	$V^{\mathrm{MNS}I}$
Type II (e leptogenesis)	$\begin{pmatrix} u_{e1} & u_{e2} \\ 0 & u_{\mu 2} \\ 0 & u_{\tau 2} \end{pmatrix}$	$\begin{pmatrix} u_{e1} & u_{e2} \\ u_{\mu 1} & 0 \\ u_{\tau 1} & 0 \end{pmatrix}$	$\begin{pmatrix} 0 & * & * \\ * & * & * \\ * & * & * \end{pmatrix}$	$\begin{pmatrix} * & * & 0 \\ * & * & * \\ * & * & * \end{pmatrix}$
Type II (μ leptogenesis)	$\begin{pmatrix} 0 & u_{e2} \\ u_{\mu 1} & u_{\mu 2} \\ 0 & u_{\tau 2} \end{pmatrix}$	$\begin{pmatrix} u_{e1} & 0 \\ u_{\mu 1} & u_{\mu 2} \\ u_{\tau 1} & 0 \end{pmatrix}$	$\begin{pmatrix} * & * & * \\ 0 & * & * \\ * & * & * \end{pmatrix}$	$\begin{pmatrix} * & * & * \\ * & * & 0 \\ * & * & * \end{pmatrix}$
Type II (τ leptogenesis)	$\begin{pmatrix} 0 & u_{e2} \\ 0 & u_{\mu 2} \\ u_{\tau 1} & u_{\tau 2} \end{pmatrix}$	$\begin{pmatrix} u_{e1} & 0 \\ u_{\mu 1} & 0 \\ u_{\tau 1} & u_{\tau 2} \end{pmatrix}$	$\begin{pmatrix} * & * & * \\ * & * & * \\ 0 & * & * \end{pmatrix}$	$\begin{pmatrix} * & * & * \\ * & * & * \\ * & * & 0 \end{pmatrix}$

III. NEUTRINO MASS SPECTRUM AND ITS MIXINGS

First we examine the neutrino mass spectrum. The eigenvalue equation for $m_{\rm eff}$ is given by $\det(m_{\rm eff} m_{\rm eff}^\dagger - \lambda) = 0$, where λ denotes the eigenvalues for the mass squared matrix and can be determined by the following equations,

$$\lambda^3 - \lambda^2 \,\mathrm{Tr}\Big(m_D \frac{1}{M} m_D^T m_D^* \frac{1}{M} m_D^\dagger\Big) + \lambda\Big(\frac{\det(m_D^\dagger m_D)}{M_1 M_2}\Big)^2 = 0. \tag{23}$$

Three mass eigenvalues of $m_{\rm eff}$ are related with the MNS matrix through the following equation,

$$V^{{\rm MNS}\dagger} m_{\rm eff} V^{{\rm MNS}*} = \begin{pmatrix} n_1 & 0 & 0 \\ 0 & n_2 & 0 \\ 0 & 0 & n_3 \end{pmatrix}. \tag{24}$$

We note that, in the minimal seesaw model with two heavy Majorana neutrinos, there are one massless neutrino and two massive neutrinos whose masses are given by

$$n_\pm^2 = \frac{X_1^2 + X_2^2 + 2X_1X_2\,\mathrm{Re}(\mathbf{u_1}^\dagger \cdot \mathbf{u_2})^2}{2} \pm \frac{\sqrt{(X_1^2 + X_2^2 + 2X_1X_2\,\mathrm{Re}(\mathbf{u_1}^\dagger \cdot \mathbf{u_2})^2)^2 - 4X_1^2X_2^2(1 - |\mathbf{u_1}^\dagger \cdot \mathbf{u_2}|^2)^2}}{2}. \tag{25}$$

For the normal hierarchical case, the mass spectrum is given by

$$\begin{aligned} n_1^2 &= 0, \qquad n_2^2 = \Delta m_{\rm sol}^2 = n_-^2, \\ n_3^2 &= \Delta m_{\rm atm}^2 + \Delta m_{\rm sol}^2 = n_+^2, \end{aligned} \tag{26}$$

and for the inverted mass hierarchical case [8], it is

$$n_1^2 = \Delta m_{\rm atm}^2 - \Delta m_{\rm sol}^2 = n_-^2, \qquad n_2^2 = \Delta m_{\rm atm}^2 = n_+^2, \qquad n_3^2 = 0. \tag{27}$$

Now, let us consider how to obtain the MNS matrix $V^{\rm MNS}$. The diagonalization of $m_{\rm eff}$ can be implemented by two steps. First, we decouple a massless state by rotating $m_{\rm eff}$ with a unitary transformation V. Then, the rotated mass matrix contains a nontrivial 2×2 part which is diagonalized by another unitary matrix K. The MNS matrix is then given by their product as follows,

$$V^{\rm MNS} = VK. \tag{28}$$

In fact, the unitary matrix V can be found from the following relations: for the normal hierarchical case, denoting it as V_N,

$$V_N^\dagger m_D = \begin{pmatrix} 0 & 0 \\ 0 & * \\ * & * \end{pmatrix}, \tag{29}$$

and for the inverted hierarchical case, denoting it as V_I,

$$V_I^\dagger m_D = \begin{pmatrix} * & * \\ 0 & * \\ 0 & 0 \end{pmatrix}. \tag{30}$$

Using the two unit vectors defined in Eq. (7), the matrix V_N and V_I can be written as

$$V_N = \left(\frac{\mathbf{u_2^*} \times \mathbf{u_1^*}}{\sqrt{1 - |\mathbf{u_1}^\dagger \cdot \mathbf{u_2}|^2}}, \quad \frac{\mathbf{u_2} - (\mathbf{u_1}^\dagger \cdot \mathbf{u_2})\mathbf{u_1}}{\sqrt{1 - |\mathbf{u_1}^\dagger \cdot \mathbf{u_2}|^2}}, \quad \mathbf{u_1} \right), \tag{31}$$

$$V_I = \left(\mathbf{u_1}, \quad \frac{\mathbf{u_2} - (\mathbf{u_1}^\dagger \cdot \mathbf{u_2})\mathbf{u_1}}{\sqrt{1 - |\mathbf{u_1}^\dagger \cdot \mathbf{u_2}|^2}}, \quad \frac{\mathbf{u_2^*} \times \mathbf{u_1^*}}{\sqrt{1 - |\mathbf{u_1}^\dagger \cdot \mathbf{u_2}|^2}} \right). \tag{32}$$

From Eqs. (29) and (30), we indeed see that a massless state is decoupled as

$$Z_N = V_N^\dagger m_{\rm eff} V_N^* = \begin{pmatrix} 0 & 0 & 0 \\ 0 & Z_{N22} & Z_{N23} \\ 0 & Z_{N23} & Z_{N33} \end{pmatrix}, \tag{33}$$

where

$$\begin{aligned} Z_{N22} &= -X_2(1 - |\mathbf{u_1}^\dagger \cdot \mathbf{u_2}|^2), \\ Z_{N33} &= -(X_1 + X_2(\mathbf{u_1}^\dagger \cdot \mathbf{u_2})^2), \\ Z_{N23} &= -X_2\sqrt{1 - |\mathbf{u_1}^\dagger \cdot \mathbf{u_2}|^2}(\mathbf{u_1}^\dagger \cdot \mathbf{u_2}). \end{aligned} \tag{34}$$

For the inverted hierarchical case,

$$V_I^\dagger m_{\rm eff} V_I^* = \begin{pmatrix} Z_{I11} & Z_{I12} & 0 \\ Z_{I12} & Z_{I22} & 0 \\ 0 & 0 & 0 \end{pmatrix}, \tag{35}$$

where

$$Z_{I11} = Z_{N33}, \qquad Z_{I12} = Z_{N23}, \qquad Z_{I22} = Z_{N22}. \tag{36}$$

Finally, the unitary matrix K is obtained from diagonalizing the 2×2 submatrix of Z. It can be parametrized by an angle θ and two phases ϕ and α. The final form for $V^{\rm MNS}$ for the normal hierarchical case is presented as

$$V_N^{\mathrm{MNS}} = \begin{pmatrix} \frac{u_{\mu 2}^* u_{\tau 1}^* - u_{\tau 2}^* u_{\mu 1}^*}{\sqrt{1-|\mathbf{u_1}^\dagger \cdot \mathbf{u_2}|^2}} & \frac{u_{e2} - u_{e1}\mathbf{u_1}^\dagger \cdot \mathbf{u_2}}{\sqrt{1-|\mathbf{u_1}^\dagger \cdot \mathbf{u_2}|^2}} & u_{e1} \\ \frac{u_{\tau 2}^* u_{e1}^* - u_{e2}^* u_{\tau 1}^*}{\sqrt{1-|\mathbf{u_1}^\dagger \cdot \mathbf{u_2}|^2}} & \frac{u_{\mu 2} - u_{\mu 1}\mathbf{u_1}^\dagger \cdot \mathbf{u_2}}{\sqrt{1-|\mathbf{u_1}^\dagger \cdot \mathbf{u_2}|^2}} & u_{\mu 1} \\ \frac{u_{e2}^* u_{\mu 1}^* - u_{\mu 2}^* u_{e1}^*}{\sqrt{1-|\mathbf{u_1}^\dagger \cdot \mathbf{u_2}|^2}} & \frac{u_{\tau 2} - u_{\tau 1}\mathbf{u_1}^\dagger \cdot \mathbf{u_2}}{\sqrt{1-|\mathbf{u_1}^\dagger \cdot \mathbf{u_2}|^2}} & u_{\tau 1} \end{pmatrix} \begin{pmatrix} 1 & 0 & 0 \\ 0 & \cos\theta_N & \sin\theta_N e^{(-i\phi_N)} \\ 0 & -\sin\theta_N e^{i\phi_N} & \cos\theta_N \end{pmatrix} \begin{pmatrix} 1 & 0 & 0 \\ 0 & e^{i\alpha_N} & 0 \\ 0 & 0 & e^{-i\alpha_N} \end{pmatrix}, \tag{37}$$

where θ_N, ϕ_N, and α_N are given as

$$\begin{aligned} \tan 2\theta_N &= \left(\frac{2|Z_{N22}^* Z_{N23} + Z_{N23}^* Z_{N33}|}{|Z_{N33}|^2 - |Z_{N22}|^2}\right), \\ &= \frac{2X_2\sqrt{1-|\mathbf{u_1}^\dagger \cdot \mathbf{u_2}|^2}|X_1(\mathbf{u_1}^\dagger \cdot \mathbf{u_2})^* + X_2 \mathbf{u_1}^\dagger \cdot \mathbf{u_2}|}{X_1^2 + X_2^2(2|\mathbf{u_1}^\dagger \cdot \mathbf{u_2}|^2 - 1) + 2X_1X_2\,\mathrm{Re}(\mathbf{u_1}^\dagger \cdot \mathbf{u_2})^2}. \\ \phi_N &= \arg(Z_{N22}^* Z_{N23} + Z_{N23}^* Z_{N33}), \\ &= \arg(X_1(\mathbf{u_1}^\dagger \cdot \mathbf{u_2})^* + X_2(\mathbf{u_1}^\dagger \cdot \mathbf{u_2})), \\ 2\alpha_N &= \arg[\cos^2\theta Z_{N22} + \sin^2\theta Z_{N33}\exp(-2i\phi) - \sin 2\theta Z_{N23}\exp(-i\phi)]. \end{aligned} \tag{38}$$

The mixing angle θ_N can be unambiguously determined by requiring the condition $\sin\theta_N \cos\theta_N \geq 0$, so that the normal mass hierarchy ($n_2^2 \leq n_3^2$) is maintained. For the inverted hierarchical case, the MNS matrix becomes

$$V_I^{\mathrm{MNS}} = \begin{pmatrix} \frac{u_{e2} - u_{e1}\mathbf{u_1}^\dagger \cdot \mathbf{u_2}}{\sqrt{1-|\mathbf{u_1}^\dagger \cdot \mathbf{u_2}|^2}} & u_{e1} & \frac{u_{\mu 2}^* u_{\tau 1}^* - u_{\tau 2}^* u_{\mu 1}^*}{\sqrt{1-|\mathbf{u_1}^\dagger \cdot \mathbf{u_2}|^2}} \\ \frac{u_{\mu 2} - u_{\mu 1}\mathbf{u_1}^\dagger \cdot \mathbf{u_2}}{\sqrt{1-|\mathbf{u_1}^\dagger \cdot \mathbf{u_2}|^2}} & u_{\mu 1} & \frac{u_{\tau 2}^* u_{e1}^* - u_{e2}^* u_{\tau 1}^*}{\sqrt{1-|\mathbf{u_1}^\dagger \cdot \mathbf{u_2}|^2}} \\ \frac{u_{\tau 2} - u_{\tau 1}\mathbf{u_1}^\dagger \cdot \mathbf{u_2}}{\sqrt{1-|\mathbf{u_1}^\dagger \cdot \mathbf{u_2}|^2}} & u_{\tau 1} & \frac{u_{e2}^* u_{\mu 1}^* - u_{\mu 2}^* u_{e1}^*}{\sqrt{1-|\mathbf{u_1}^\dagger \cdot \mathbf{u_2}|^2}} \end{pmatrix} \begin{pmatrix} \cos\theta_I & \sin\theta_I e^{(-i\phi_I)} & 0 \\ -\sin\theta_I e^{i\phi_I} & \cos\theta_I & 0 \\ 0 & 0 & 1 \end{pmatrix} \begin{pmatrix} e^{i\alpha_I} & 0 & 0 \\ 0 & e^{-i\alpha_I} & 0 \\ 0 & 0 & 1 \end{pmatrix}, \tag{39}$$

where θ_I, ϕ_I, and α_I have the same expressions as the normal hierarchical case given in terms of X_1, X_2, $\mathbf{u_1}$, and $\mathbf{u_2}$. The condition $\sin\theta_I \cos\theta_I \geq 0$ ($n_1^2 \leq n_2^2$) is required for the inverted hierarchical case. Having established how to construct the MNS matrix, we study the flavor mixings of two zeros texture models which are discussed in the previous section. We first study zero of MNS matrix elements of type II models. The type II models predict that one of the MNS matrix elements is zero. Because experimental constraints allow $|V_{e3}^{\mathrm{MNS}}|$ to be vanishing, among type II models, only e leptogenesis and the inverted hierarchical case is allowed. About the type I models, in general, we do not have zero of the MNS matrix elements. Therefore, we need to carry out the detailed numerical study on the mixing angles, which will be presented in the next section.

IV. NUMERICAL ANALYSIS

A. Determination of parameters

From neutrino oscillation experiments, two mixing angles, the upper bound on $|V_{e3}^{\mathrm{MNS}}|$, and two neutrino mass squared differences have been determined [13,14], which are taken as inputs. Because in models with two zeros for m_D, the effective low energy mass matrix m_{eff} can be presented in terms of five independent parameters including a CP phase, all these parameters can be severely constrained from the experimental results mentioned above. In this class of models, the allowed ranges for V_{e3}^{MNS} and the Jarlskog invariant J [12] may be predicted. In this section, we determine the allowed ranges for the parameters and predict $|V_{e3}^{\mathrm{MNS}}|$ and CP violation in neutrino oscillations $|J|$. Based on this analysis, we can construct the possible forms of the unitarity triangle of the leptonic sector. We first show how two parameters X_1 and X_2 with mass dimensions can be fixed by using Δm^2 and $\mathbf{u_1}^\dagger \cdot \mathbf{u_2}$ as inputs. Writing $\mathbf{u_1}^\dagger \cdot \mathbf{u_2}$ as

$$\mathbf{u}_1^\dagger \cdot \mathbf{u_2} = \cos\beta e^{i\gamma}, \tag{40}$$

where $0 \leq \cos\beta$ and $-\pi \leq \gamma \leq \pi$, and using Eq. (25), we can write $X_1 + X_2$ and $|X_1 - X_2|$ as

$$\begin{aligned} X_1 + X_2 &= \sqrt{n_+^2 + n_-^2 + 2n_+n_-\cos 2\gamma + \frac{4n_+n_-}{\sin^2\beta}\sin^2\gamma}, \\ |X_1 - X_2| &= \sqrt{n_+^2 + n_-^2 + 2n_+n_-\cos 2\gamma - \frac{4n_+n_-}{\sin^2\beta}\cos^2\gamma}. \end{aligned} \tag{41}$$

Choosing either $X_1 \leq X_2$ or $X_1 \geq X_2$, we may write X_1 and X_2 in terms of β, γ, and neutrino masses. [See Eqs. (26)

and (27)]. For numerical analysis, we use $\Delta m^2_{\rm sol} = 7.1 \times 10^{-5}$ (eV^2) and $\Delta m^2_{\rm atm} = 2.6 \times 10^{-3}$ (eV^2). Here, we note that the inputs $(\beta, \gamma, \Delta m^2_{\rm sol}, \Delta m^2_{\rm atm})$ are sufficient for determining $\sin\theta_{N,I}$ and $\phi_{N,I}$ in K with the help of Eq. (38). We also note that $\cos\beta$ is bounded as

$$\cos\beta \leq \frac{(n_+ - n_-)}{\sqrt{n_+^2 + n_-^2 + 2n_+n_- \cos 2\gamma}}. \tag{42}$$

Next we illustrate how one can fit the models with two zeros in m_D by using the experimental results. As an example, we take the type I(a) τ-leptogenesis model which is listed in Table I. In the model, $u_{\tau 1}$, u_{e1}, and $u_{\mu 2}$ can be taken to be real and positive and $u_{\tau 2}$ is a complex variable. From the τ-leptogenesis assumption,

$$u_{\tau 1} u_{\tau 2} = \cos\beta \exp(i\gamma). \tag{43}$$

By considering the range of the parameters, $\cos\beta \leq u_{\tau 1} \leq 1$, $|\gamma| \leq \pi$, one can numerically generate $u_{\tau 1}$, γ, and β as

$$\begin{aligned} u_{\tau 1} &= \cos\beta + \frac{k}{N_k}(1 - \cos\beta) \quad (k = 0 \sim N_k), \\ \gamma &= -\pi + 2\frac{(n_g - 1)\pi}{N_g} \quad (n_g = 1 \sim N_g), \\ \beta &= \frac{(n_\beta - 1)\pi}{2N_\beta} \quad (n_\beta = 1 \sim N_\beta), \end{aligned} \tag{44}$$

where the number of divisions for each variable are taken to be $N_\beta = N_g = 50$ and $N_k = 10$. Then, we generate $(N_k + 1)N_g N_\beta$ sets of $(\beta, \gamma, u_{\tau 1})$. The other parameters in u_{ai} can be determined as

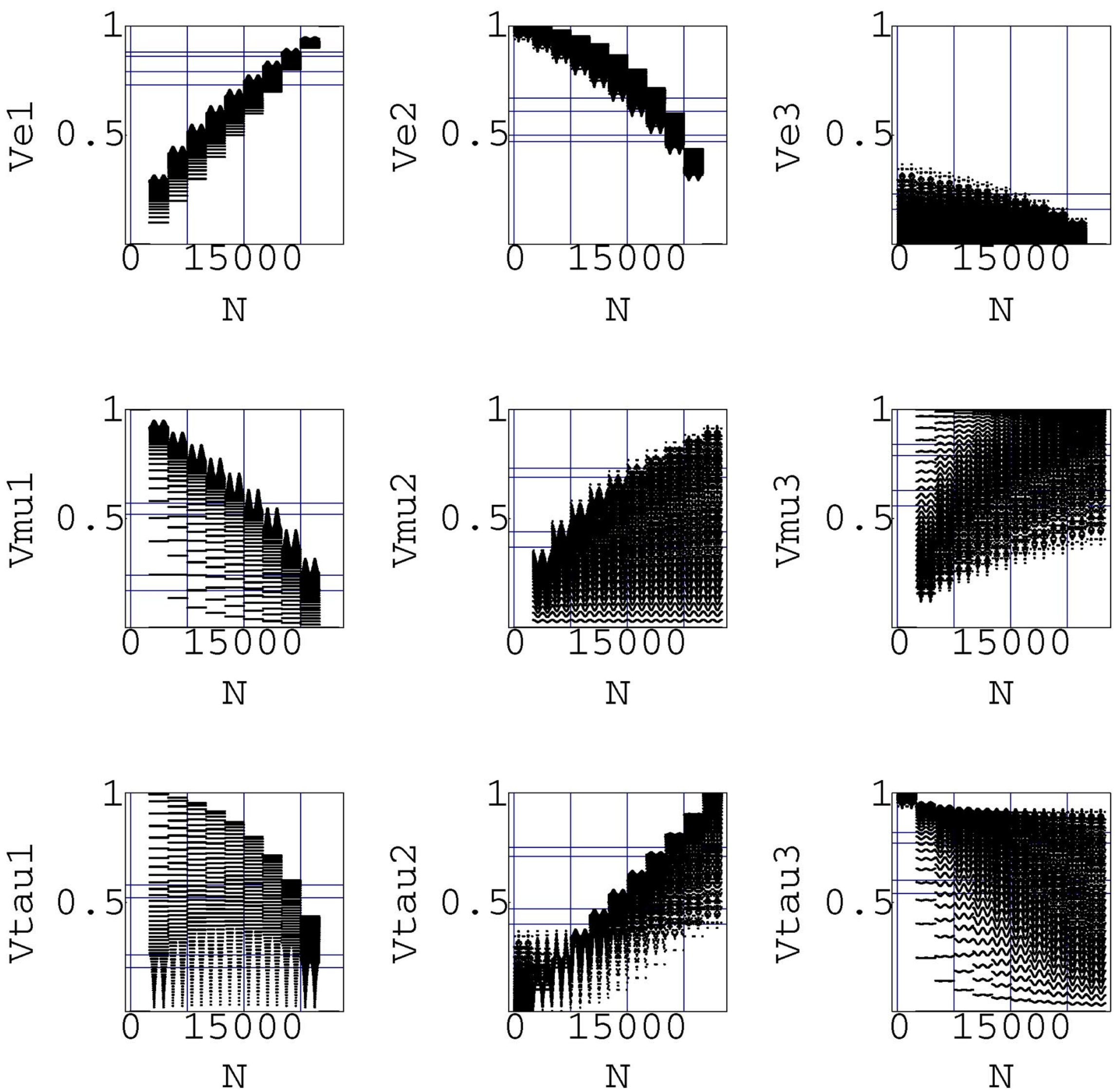

FIG. 2 (color online). $|V^{\rm MNS}_{ij}|$ for τ-leptogenesis model type I(a) with normal hierarchy and $X_1 \leq X_2$.

$$u_{\tau 2} = \frac{\cos\beta \exp(i\gamma)}{u_{\tau 1}}, \qquad u_{e1} = \sqrt{1 - |u_{\tau 1}|^2}, \qquad u_{\mu 2} = \sqrt{1 - |u_{\tau 2}|^2}. \tag{45}$$

By fixing the parameters $(\beta, \gamma, u_{\tau 1})$, which is equivalent to giving a set of three integers (n_β, n_g, k), we can generate all the elements of the MNS matrix through Eqs. (37)–(41) and (45). To show how we determine the parameters by taking into account the experimental constraints, it is convenient to represent a set of the integers (n_β, n_g, k) with an integer N defined as

$$N = kN_\beta N_g + (n_g - 1)N_\beta + n_\beta. \tag{46}$$

For a given N, one can extract a set of three integer numbers (n_β, n_g, k) as follows,

$$k = \left[\frac{N}{N_g N_\beta}\right], \qquad N' = \mathrm{Mod}.[N, N_g N_\beta], \qquad n_g = \left[\frac{N'}{N_\beta}\right] + 1, \qquad n_\beta = \mathrm{Mod}.[N', N_\beta], \tag{47}$$

where $[x]$ denotes the maximum integer which is not larger than x. By taking N in the horizontal axis, we show the prediction for the absolute values of MNS matrix elements in the vertical axis as shown in Fig. 2. A point of the horizontal axis corresponds to a set of parameters for $(\beta, \gamma, u_{\tau 1})$. We also show the experimentally allowed range for MNS matrix elements both at 90% confidence level and at 3σ level taken from [14]. One can find N which leads to the MNS matrix elements consistent with experiments. Then, we can determine (n_β, n_g, k) by Eq. (47) and $(\beta, \gamma, u_{\tau 1})$ by Eq. (45), respectively. In Fig. 3, we show

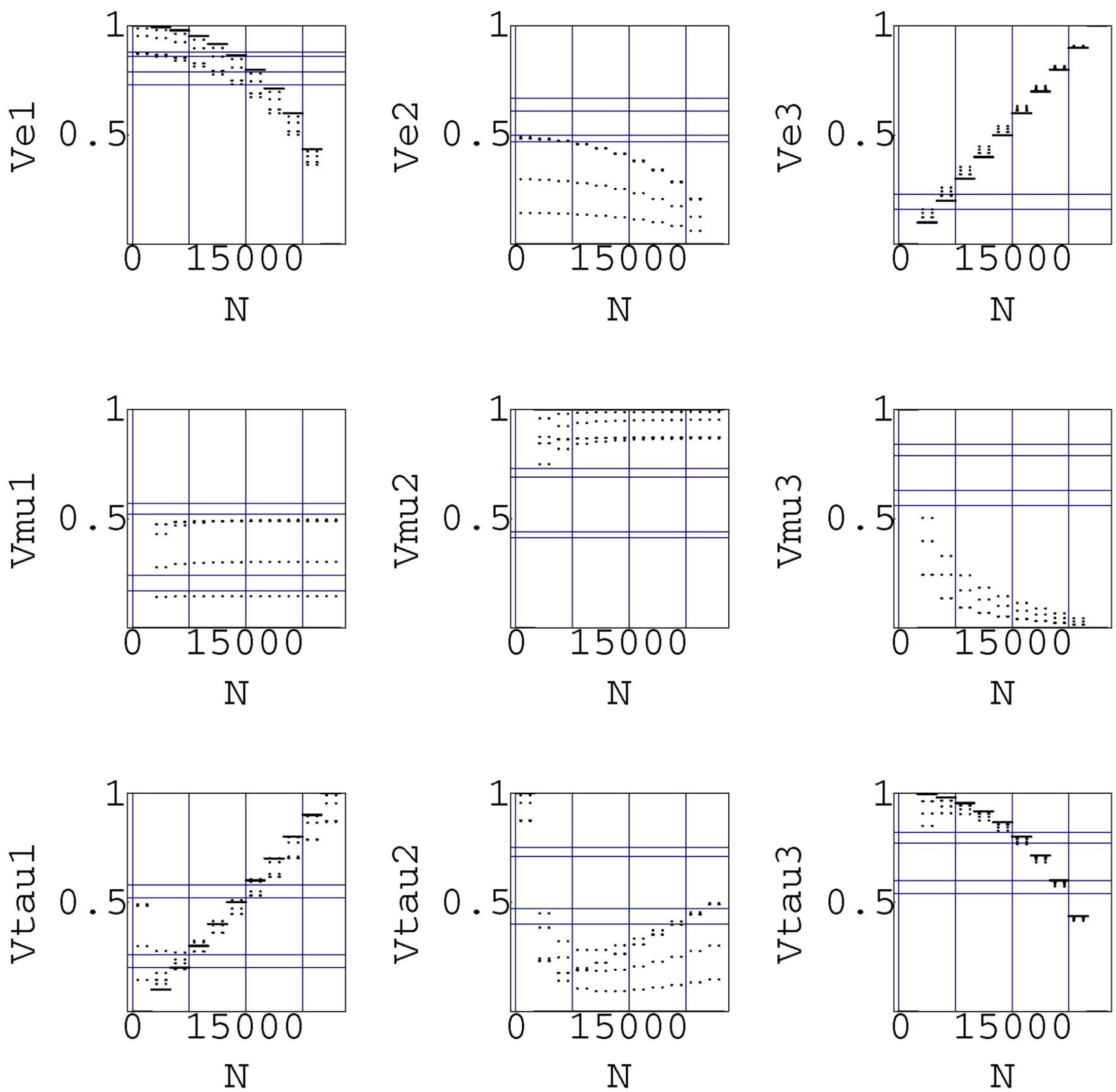

FIG. 3 (color online). $|V_{ij}^{\mathrm{MNS}}|$ for τ-leptogenesis model type I(a) with inverted hierarchy and $X_1 \leq X_2$.

TABLE III. The predictions for $|V_{ij}^{\mathrm{MNS}}|$ and $|J|$. The magnitudes of the V_{ij}^{MNS} given in the second row correspond to experimental constraints at 90% C.L. taken from [14].

Type	$\lvert V_{e1}^{\mathrm{MNS}}\rvert$	$\lvert V_{e2}^{\mathrm{MNS}}\rvert$	$\lvert V_{e3}^{\mathrm{MNS}}\rvert$	$\lvert V_{\mu 3}^{\mathrm{MNS}}\rvert$	$\lvert V_{\tau 3}^{\mathrm{MNS}}\rvert$	$\lvert J\rvert$
Exp. (90%)	$0.79 \sim 0.86$	$0.50 \sim 0.61$	$0 \sim 0.16$	$0.63 \sim 0.79$	$0.60 \sim 0.77$	
I(a) μ normal $X_1 \leq X_2$	$0.79 \sim 0.86$	$0.50 \sim 0.61$	$0.058 \sim 0.11$	$0.63 \sim 0.79$	$0.60 \sim 0.77$	$0 \sim 0.023$
I(b) μ normal $X_2 \leq X_1$	$0.79 \sim 0.86$	$0.50 \sim 0.61$	$0.058 \sim 0.11$	$0.64 \sim 0.79$	$0.61 \sim 0.77$	$0 \sim 0.024$
I(a) τ normal $X_1 \leq X_2$	$0.79 \sim 0.86$	$0.50 \sim 0.61$	$0.054 \sim 0.10$	$0.63 \sim 0.79$	$0.61 \sim 0.77$	$0 \sim 0.022$
I(b) τ normal $X_2 \leq X_1$	$0.79 \sim 0.86$	$0.50 \sim 0.61$	$0.054 \sim 0.10$	$0.63 \sim 0.79$	$0.61 \sim 0.77$	$0 \sim 0.022$

TABLE IV. The predictions for $|V_{ij}^{\mathrm{MNS}}|$ and $|J|$. The magnitudes of the V_{ij}^{MNS} given in the second row correspond to experimental constraints at 3σ taken from [14].

Type	$\lvert V_{e1}^{\mathrm{MNS}}\rvert$	$\lvert V_{e2}^{\mathrm{MNS}}\rvert$	$\lvert V_{e3}^{\mathrm{MNS}}\rvert$	$\lvert V_{\mu 3}^{\mathrm{MNS}}\rvert$	$\lvert V_{\tau 3}^{\mathrm{MNS}}\rvert$	$\lvert J\rvert$
Exp. (3σ)	$0.73 \sim 0.88$	$0.47 \sim 0.67$	$0 \sim 0.23$	$0.56 \sim 0.84$	$0.54 \sim 0.82$	
I(a) μ normal $X_1 \leq X_2$	$0.73 \sim 0.88$	$0.47 \sim 0.67$	$0.046 \sim 0.13$	$0.57 \sim 0.83$	$0.54 \sim 0.82$	$0 \sim 0.028$
I(b) μ normal $X_2 \leq X_1$	$0.73 \sim 0.88$	$0.47 \sim 0.67$	$0.047 \sim 0.13$	$0.57 \sim 0.83$	$0.54 \sim 0.82$	$0 \sim 0.028$
I(a) τ normal $X_1 \leq X_2$	$0.73 \sim 0.88$	$0.47 \sim 0.67$	$0.044 \sim 0.13$	$0.56 \sim 0.84$	$0.54 \sim 0.82$	$0 \sim 0.027$
I(b) τ normal $X_2 \leq X_1$	$0.73 \sim 0.88$	$0.47 \sim 0.67$	$0.043 \sim 0.12$	$0.56 \sim 0.84$	$0.54 \sim 0.82$	$0 \sim 0.027$
I(a) μ inverted $X_1 \leq X_2$	$0.86 \sim 0.87$	$0.48 \sim 0.49$	$0.027 \sim 0.14$	$0.63 \sim 0.82$	$0.56 \sim 0.77$	$0.0055 \sim 0.027$
I(b) μ inverted $X_2 \leq X_1$	$0.86 \sim 0.87$	$0.48 \sim 0.49$	$0.022 \sim 0.14$	$0.57 \sim 0.84$	$0.54 \sim 0.82$	$0.0044 \sim 0.028$
I(a) τ inverted $X_1 \leq X_2$	$0.86 \sim 0.87$	$0.48 \sim 0.49$	$0.027 \sim 0.13$	$0.59 \sim 0.84$	$0.54 \sim 0.80$	$0.0055 \sim 0.026$
I(b) τ inverted $X_2 \leq X_1$	$0.86 \sim 0.87$	$0.48 \sim 0.49$	$0.021 \sim 0.13$	$0.57 \sim 0.84$	$0.55 \sim 0.82$	$0.0039 \sim 0.027$
II(a) e inverted $X_1 \leq X_2$	0.87	$0.49 \sim 0.50$	0	$0.57 \sim 0.84$	$0.55 \sim 0.82$	0
II(b) e inverted $X_2 \leq X_1$	0.87	$0.49 \sim 0.50$	0	$0.57 \sim 0.84$	$0.55 \sim 0.82$	0

the fit for the inverted hierarchical case. By finding N which reproduces the magnitude of five MNS matrix elements simultaneously, we can determine the parameters of the model. In this way, one can find N which puts MNS matrix elements within the experimentally allowed range. In Table III, we show our fit based on the experimental determination of the mixing angles at 90% C.L. Only four types of textures are allowed and all the types correspond to the normal hierarchical case and either the μ- or τ-leptogenesis case. $|V_{e3}^{\mathrm{MNS}}|$ is determined to be nonzero and the upper bound for CP violation $|J|$ is obtained. In Table IV, we relax experimental constraints by using the 3σ allowed range. In this case, more textures are allowed and the allowed ranges are larger than the previous case. In addition to the previous allowed textures, the type II e-leptogenesis (inverted hierarchical) case is allowed. As for the type I μ and τ leptogenesis, the inverted hierachical cases can also be fitted. Let us summarize the fitted results for each texture as follows.

(i) Type II e-leptogenesis scenarios. In this class of models, because $|V_{e3}^{\mathrm{MNS}}| = 0$, CP violation in neutrino oscillation J is vanishing in spite of nonzero γ.

(ii) Type I μ and τ leptogenesis for the normal hierarchical case. In this class of models, V_{e3}^{MNS} is nonvanishing. About the CP violation phase, the allowed range of $|J|$ is from zero to some nonvanishing value.

(iii) Type I μ and τ leptogenesis for the inverted hierarchical case. In this class of models, both V_{e3}^{MNS} and $|J|$ are nonvanishing.

B. $|V_{e3}^{\mathrm{MNS}}|$ versus $|J|$

To clarify the differences of predictions between the inverted hierarchical case and the normal hierarchical case, we have plotted $|V_{e3}^{\mathrm{MNS}}|$ versus $|J|$ in Figs. 4–6. When $|V_{e3}^{\mathrm{MNS}}| \ll 1$, J is approximately proportional to $|V_{e3}^{\mathrm{MNS}}|$. By choosing the standard parametrization of the MNS matrix, we obtain

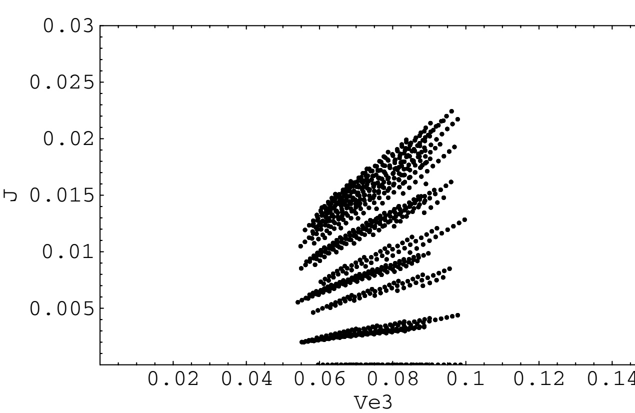

FIG. 4. $|J|$ and $|V_{e3}^{\mathrm{MNS}}|$ for τ-leptogenesis model type I(a) with normal hierarchy and $X_1 \leq X_2$ (90%).

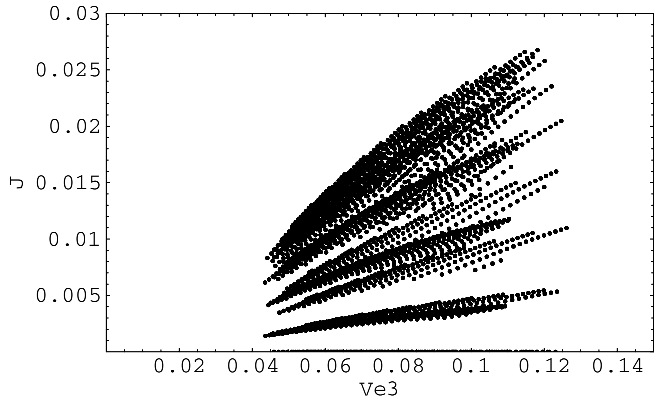

FIG. 5. $|J|$ and $|V_{e3}^{\mathrm{MNS}}|$ for τ-leptogenesis model type I(a) with normal hierarchy and $X_1 \leq X_2$ (3σ).

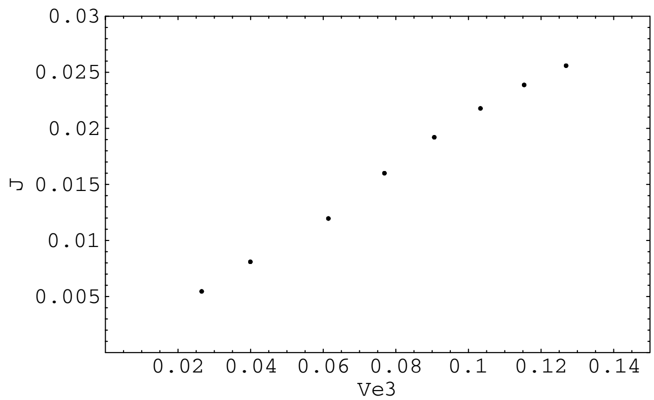

FIG. 6. $|J|$ and $|V_{e3}^{\mathrm{MNS}}|$ for τ-leptogenesis model type I(a) with inverted hierarchy and $X_1 \leq X_2$ (3σ).

$$J = (1 - s_{13}^2)s_{13}c_{12}s_{12}c_{23}s_{23}\sin\delta, \tag{48}$$

with $V_{e3}^{\mathrm{MNS}} = s_{13}\exp(-i\delta)$. In Figs. 4–6, within good approximation, we can find the linear correlation between $|J|$ and $|V_{e3}^{\mathrm{MNS}}|$. One can read $|\sin\delta|$ from the slope since

$$|\sin\delta| \simeq \frac{1}{c_{12}s_{12}c_{23}s_{23}}\frac{|J|}{s_{13}}. \tag{49}$$

In type I models with normal hierarchy, μ and τ leptogenesis are allowed. The allowed range for $\sin\delta$ is

$$0 \leq |\sin\delta| \lesssim 1. \tag{50}$$

For type I with inverted hierarchy, $\sin\delta$ is almost maximal,

$$|\sin\delta| \simeq 1, \tag{51}$$

which implies that the CP violating phase γ takes some nonvanishing definite value. By fitting the data of neutrino mixings, we have determined the allowed ranges for the parameters which are presented in Table V.

C. Unitarity triangle

Further, one can reconstruct the unitarity triangles of the models with two zeros texture which can satisfy the experimental constraints. We focus on the unitarity triangle of the $\mu - e$ sector,

$$\begin{aligned} &V_{e1}^{\mathrm{MNS}}V_{\mu1}^{\mathrm{MNS}*} + V_{e2}^{\mathrm{MNS}}V_{\mu2}^{\mathrm{MNS}*} + V_{e3}^{\mathrm{MNS}}V_{\mu3}^{\mathrm{MNS}*} = 0,\\ &V_{e1}^{\mathrm{MNS}}V_{\mu1}^{\mathrm{MNS}*} = -c_{13}(c_{12}s_{12}c_{23} + c_{12}^2s_{23}s_{13}\exp(-i\delta)),\\ &V_{e2}^{\mathrm{MNS}}V_{\mu2}^{\mathrm{MNS}*} = c_{13}(s_{12}c_{12}c_{23} - s_{12}^2s_{23}s_{13}\exp(-i\delta)),\\ &V_{e3}^{\mathrm{MNS}}V_{\mu3}^{\mathrm{MNS}*} = +c_{13}s_{13}s_{23}\exp(-i\delta). \end{aligned} \tag{52}$$

First we show the triangle schematically in Fig. 7. The

TABLE V. The parameters which are determined by fitting with mixing angles. The values in parentheses are obtained from the magnitudes of MNS elements corresponding to a 3σ fit taken from [14]. The others correspond to 90% C.L. fit in [14].

			$\lvert\gamma\rvert$	β
II(a) e inverted $X_1 \leq X_2$	$(0.30) \leq \lvert u_{\mu2}\rvert^2 \leq (0.67)$	$(0.33) \leq \lvert u_{\tau2}\rvert^2 \leq (0.70)$	$(1.4) \sim (1.8)$	(1.5)
II(b) e inverted $X_1 \geq X_2$	$(0.30) \leq \lvert u_{\mu1}\rvert^2 \leq (0.67)$	$(0.33) \leq \lvert u_{\tau1}\rvert^2 \leq (0.70)$	$(1.4) \sim (1.8)$	(1.5)
I(a) μ normal $X_1 \leq X_2$	$0.085 \leq \lvert u_{e1}\rvert^2 \leq 0.29$	$0.24 \leq \lvert u_{\tau2}\rvert^2 \leq 0.68$	$0 \sim 3.1$	$0.60 \sim 1.1$
	$(0.050) \leq \lvert u_{e1}\rvert^2 \leq (0.37)$	$(0.16) \leq \lvert u_{\tau2}\rvert^2 \leq (0.75)$	$(0) \sim (3.1)$	$(0.47) \sim (1.1)$
I(a) μ inverted $X_1 \leq X_2$	$(0.97) \leq \lvert u_{e1}\rvert^2 \leq (1.0)$	$(0.40) \leq \lvert u_{\tau2}\rvert^2 \leq (0.68)$	$(1.4) \sim (1.8)$	(1.5)
I(b) μ normal $X_1 \geq X_2$	$0.25 \leq \lvert u_{\tau1}\rvert^2 \leq 0.68$	$0.082 \leq \lvert u_{e2}\rvert^2 \leq 0.29$	$0 \sim 3.1$	$0.60 \sim 1.1$
	$(0.16) \leq \lvert u_{\tau1}\rvert^2 \leq (0.75)$	$(0.050) \leq \lvert u_{e2}\rvert^2 \leq (0.37)$	$(0) \sim (3.1)$	$(0.47) \sim (1.1)$
I(b) μ inverted $X_1 \geq X_2$	$(0.33) \leq \lvert u_{\tau1}\rvert^2 \leq (0.70)$	$(0.97) \leq \lvert u_{e2}\rvert^2 \leq (1.0)$	$(1.4) \sim (1.8)$	(1.5)
I(a) τ normal $X_1 \leq X_2$	$0.093 \leq \lvert u_{e1}\rvert^2 \leq 0.29$	$0.28 \leq \lvert u_{\mu2}\rvert^2 \leq 0.71$	$0 \sim 3.1$	$0.63 \sim 1.1$
	$(0.054) \leq \lvert u_{e1}\rvert^2 \leq (0.38)$	$(0.18) \leq \lvert u_{\mu2}\rvert^2 \leq (0.78)$	$(0) \sim (3.1)$	$(0.50) \sim (1.2)$
I(a) τ inverted $X_1 \leq X_2$	$(0.98) \leq \lvert u_{e1}\rvert^2 \leq (1.0)$	$(0.30) \leq \lvert u_{\mu2}\rvert^2 \leq (0.64)$	$(1.4) \sim (1.8)$	(1.5)
I(b) τ normal $X_1 \geq X_2$	$0.28 \leq \lvert u_{\mu1}\rvert^2 \leq 0.71$	$0.092 \leq \lvert u_{e2}\rvert^2 \leq 0.29$	$0 \sim 3.1$	$0.63 \sim 1.1$
	$(0.18) \leq \lvert u_{\mu1}\rvert^2 \leq (0.78)$	$(0.054) \leq \lvert u_{e2}\rvert^2 \leq (0.37)$	$(0) \sim (3.1)$	$(0.50) \sim (1.2)$
I(b) τ inverted $X_1 \geq X_2$	$(0.30) \leq \lvert u_{\mu1}\rvert^2 \leq (0.67)$	$(0.97) \leq \lvert u_{e2}\rvert^2 \leq (1.0)$	$(1.4) \sim (1.8)$	(1.5)

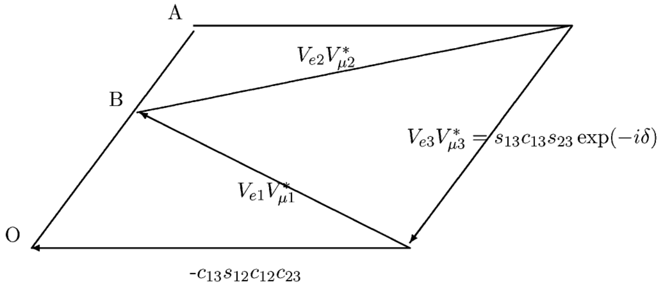

FIG. 7. Schematic view of unitarity triangle.

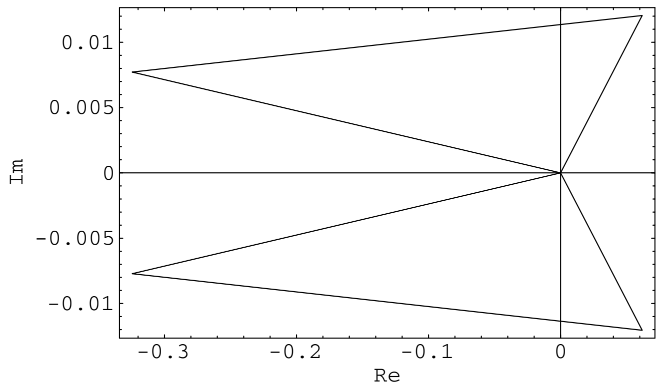

FIG. 8. Unitarity triangles for τ-leptogenesis model type I(a) with normal hierarchy which correspond to $|V_{e1}| \simeq 0.80$, $|V_{e2}| \simeq 0.60$, $|V_{e3}| \simeq 0.098$, $|V_{\mu 1}| \simeq 0.41$, $|V_{\mu 2}| \simeq 0.65$, $|V_{\mu 3}| \simeq 0.64$, $|V_{\tau 3}| \simeq 0.76$, $|J| \simeq 0.0044$, $|\sin\delta| \simeq 0.19$, $|\gamma| \simeq 3.0$, and $\beta \simeq 0.94$.

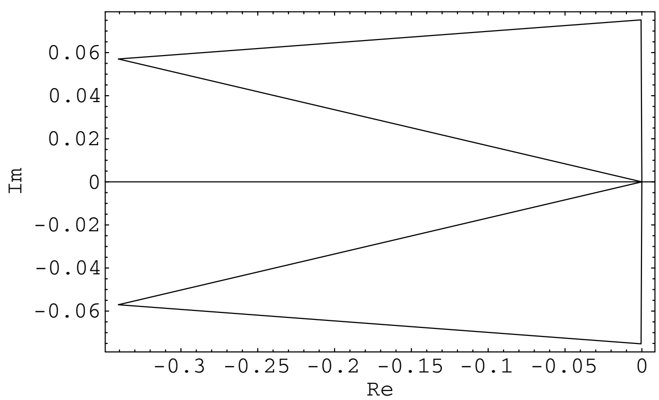

FIG. 9. Unitarity triangles for τ-leptogenesis model type I(a) with inverted hierarchy which correspond to $|V_{e1}| \simeq 0.86$, $|V_{e2}| \simeq 0.49$, $|V_{e3}| \simeq 0.13$, $|V_{\mu 1}| \simeq 0.40$, $|V_{\mu 2}| \simeq 0.70$, $|V_{\mu 3}| \simeq 0.59$, $|V_{\tau 3}| \simeq 0.80$, $|J| \simeq 0.026$, $|\sin\delta| \simeq 1.0$, $|\gamma| \simeq 1.6$, and $\beta \simeq 1.5$.

triangle can be drawn inside a parallelogram as shown in Fig. 7. We note that

$$\mathrm{OB}:\mathrm{AB} = \mathrm{c}_{12}^2:\mathrm{s}_{12}^2, \tag{53}$$

and δ is the argument between V_{e3}^{MNS} and the real axis. In Figs. 8 and 9, we have shown the triangle corresponding to the type I(a) τ leptogenesis for the normal and inverted hierarchical cases, respectively. As we have already noted, the inverted hierarchical case $\sin\delta$ is almost maximal. Therefore the argument of V_{e3} with respect to the real axis is 90°. For the normal hierarchical case, $|\sin\delta|$ is smaller than 1. Because only the magnitude of V^{MNS} is known, we have two-fold ambiguities for δ even if the sizes of s_{12}, s_{23}, $|V_{e3}^{\mathrm{MNS}}|$, and $|J|$ are given. In Fig. 8, we plot two triangles which correspond to δ and $-\delta$. Two triangles which are related to each other by reflection with respect to the real axis can be distinguished by measuring the sign of J.

V. SUMMARY AND DISCUSSIONS

In this work, we study *CP* violation in neutrino oscillations and its possible connection to lepton family asymmetries generated from heavy Majorana neutrino decays. We have derived a general formula for *CP* violation in neutrino oscillations by means of heavy Majorana masses and the Dirac mass matrix. We identify the two zeros texture models in which lepton asymmetry is dominated by a particular family asymmetry. We have explored the e-leptogenesis, μ-leptogenesis, and τ-leptogenesis scenarios and determined the allowed range of parameters from the neutrino experimental results. Using the 90% and 3σ bound on the magnitude of mixing angles measured at experiments, we have constrained the parameters of the models. Based on the analysis above, we have predicted the possible ranges of $|V_{e3}^{\mathrm{MNS}}|$ and the low energy *CP* violation observable $|J|$. We have found that in the models with two zeros in m_D and inverted hierarchy, $|\sin\delta|$ is predicted to be almost maximal. Once those two unknown quantities are determined in future neutrino oscillation experiments, we could compare them with our predictions. Because the sign of J would be determined from the measurement of *CP* violation via neutrino oscillations, we can conclude whether the sign of *CP* violation at low energy is consistent with *CP* violation required in cosmology [3,5,7].

ACKNOWLEDGMENTS

We thank Z. Xiong and Z. Xing for discussions. We also thank the Yukawa Institute for Theoretical Physics at Kyoto University, where this work was initiated during the workshop YITP-W-04-08 on "Summer Institute 2004" and YITP-W-04-21 on "*CP* Violation and Matter and Anti-matter Asymmetry." This work is supported by the kakenhi of MEXT, Japan, No. 16028213 (T. M.). S. K. K. is supported in part by the BK21 program of the Ministry of Education in Korea and in part by KOSEF Grant No. R01-2003-000-10229-0.

[1] M. Fukugita and T. Yanagida, Phys. Lett. B **174**, 45 (1986).

[2] T. Endoh, T. Morozumi, A. Purwanto, and T. Onogi, Phys. Rev. D **64**, 013006 (2001); **64**, 059904 (2001).

[3] G. C. Branco, T. Morozumi, B. Nobre, and M. N. Rebelo, Nucl. Phys. **B617**, 475 (2001).

[4] T. Endoh, T. Morozumi, and Z. Xiong, Prog. Theor. Phys. **111**, 123 (2004).

[5] P. H. Frampton, S. L. Glashow, and T. Yanagida, Phys. Lett. B **548**, 119 (2002).

[6] W. Buchmuller, P. Di Bari, and M. Plumacher, Ann. Phys. (N.Y.) **315**, 305 (2005).

[7] T. Endoh, S. Kaneko, S. K. Kang, T. Morozumi, and M. Tanimoto, Phys. Rev. Lett. **89**, 231601 (2002).

[8] W. Guo and Z. Xing, Phys. Lett. B **583**, 163 (2004).

[9] Z. Xing, Phys. Rev. D **69**, 013006 (2004).

[10] R. N. Mohapatra and S. Nasri, Phys. Rev. D **71**, 033001 (2005).

[11] L. Covi, E. Roulet, and F. Vissani, Phys. Lett. B **384**, 169 (1996).

[12] C. Jarlskog, Phys. Rev. Lett. **55**, 1039 (1985).

[13] M. Fukugita and M. Tanimoto, Phys. Lett. B **515**, 30 (2001).

[14] M. C. Gonzalez-Garcia and C. Pena-Garay, Phys. Rev. D **68**, 093003 (2003).